

## Article

# Determining the Geogenic Radon Potential in Different Layouts and Numbers of Points

Alexandru Lupulescu <sup>1,\*</sup>, Călin Baciuc <sup>1</sup>, Tiberius Dicu <sup>1</sup>, Bety-Denissa Burghele <sup>1,2</sup>  
and Alexandra Laura Cucos <sup>1</sup>

<sup>1</sup> Centre of Applied Environmental Research, Faculty of Environmental Science and Engineering, Babeş-Bolyai University, Fântânele 30, 400535 Cluj-Napoca, Romania

<sup>2</sup> SC Radon Action SRL, Str. Mărginaşă 51, 400371 Cluj-Napoca, Romania

\* Correspondence: alexandru.lupulescu@ubbcluj.ro

**Abstract:** The geogenic radon potential is primarily controlled by the geological characteristics of the site, such as the rock type and structural elements, as well as the permeability of the soil. Depending on the scope of the survey, the geogenic radon potential can be mapped based on measurements conducted in the field at various resolutions. Detailed surveys are generally labour-intensive and time-consuming. Therefore, a balance should be reached between the desired level of precision and the required amount of effort, delivering the best results with the least number of resources. The international literature describes a variety of surveying techniques. This study was undertaken in a region of the central zone of the Poiana Rusca Mountains (Southern Carpathians, Romania) that contains several metamorphic, volcanic, and sedimentary rock types. The primary objective of the study is to compare alternative sampling point configurations, which vary in number and arrangement. The objective was to achieve the most accurate representation of the calculated geogenic radon potential while limiting the number of measurements and the time and effort associated with them. Radon activity concentration and soil permeability data were collected from 34 locations using seven alternative layouts of the sampling points. The proposed layouts were based on various configurations of fifteen, nine, five, and three sampling points. Locally, in some of the metamorphic units and in the regions containing sedimentary deposits with volcanic intercalations, the geogenic radon potential was found to be elevated. The results indicate that the three-measuring-point configuration is acceptable for general geogenic radon potential surveys.

**Keywords:** geogenic radon potential; soil permeability; natural radioactivity; radon



**Citation:** Lupulescu, A.; Baciuc, C.; Dicu, T.; Burghele, B.-D.; Cucos, A.L. Determining the Geogenic Radon Potential in Different Layouts and Numbers of Points. *Atmosphere* **2023**, *14*, 713. <https://doi.org/10.3390/atmos14040713>

Academic Editor: Antoaneta Ene

Received: 13 March 2023

Revised: 2 April 2023

Accepted: 12 April 2023

Published: 14 April 2023



**Copyright:** © 2023 by the authors. Licensee MDPI, Basel, Switzerland. This article is an open access article distributed under the terms and conditions of the Creative Commons Attribution (CC BY) license (<https://creativecommons.org/licenses/by/4.0/>).

## 1. Introduction

Radon-222 is a radioactive gas directly produced by the decay of radium (<sup>226</sup>Ra) in the natural uranium decay series. The radon levels inside buildings are determined by the geology of the region, the construction materials, the presence of a basement or cellar, and the occupants' way of life [1,2]. Radon has been regarded as a hazardous gas for a long time [3], which has driven national and international efforts to map and control radon [4,5]. It is generally accepted that soil is the primary source of radon indoors [6]. The potential for radon in soil and indoor environments is mostly influenced by the underlying geology of the region [7–9].

Geogenic radon potential (GRP) is defined as “what earth delivers” in terms of radon. Radioactive elements from the family of radium isotopes, contained in mineral particles from soil and underlying rocks, may release radon, which will concentrate in the soil pores. Depending on the soil's permeability, the soil gas mixture may migrate upwards to the soil's surface [10]. Depending on the original bedrock, the number of radioactive elements in the Earth's crust can vary substantially [11]. To evaluate the geogenic radon potential, radon activity concentration in soil and soil permeability must be measured, notwithstanding the

availability of bedrock data. In different countries, GRP has been evaluated using a variety of methodologies, making macro-level data corroboration challenging [12]. Some examples are given below.

In the Czech Republic, Neznal et al. [13] proposed a method utilising 15 sample locations per 800 m<sup>2</sup> of soil surface for construction development. The method is hereafter identified as the Neznal method. The soil radon concentration was measured using Lucas cells, while the soil permeability was evaluated using a Radon Jok device (Radon v.o.s., Prague, Czech Republic). Radon potential (RP) was transformed into radon index (RI), which indicates the level of radon risk given by the bedrock. The authors developed a classification of radon index depending on the radon potential of the building site, as follows: RI is low when  $RP < 10$ ; RI is medium when  $10 \leq RP < 35$ ; and RI is high when  $RP \geq 35$ . Mikšová & Barnet [14] measured the soil radon concentration in the Czech Republic National Radon Program. Emanometers based on the ionisation chamber or Lucas cells principle and the portable instrument Scintrex RDA 200 were used. The samples for radon concentration in the soil were collected at a depth of 0.8 m. Soil permeability was measured in situ, or it was determined by granulometric analysis of the soil.

In Hungary, Szabó et al. [15] employed the equation developed by Neznal et al. [13] for GRP calculation using a single measuring point. In this case, however, soil radon concentration measurements were conducted using a RAD7 instrument (DurrIDGE Company Inc., Billerica, MA, USA). Soil permeability was determined using the Radon Jok device.

In Croatia, Planinić et al. [16] used LR-115 detectors in order to determine the soil radon concentration. These detectors were placed at a depth of 0.5 m for a period of one week. Two detectors were used for each location, thus obtaining the arithmetic mean for the two values of radon concentrations in the soil.

Chalupnik & Wysocka's [17] study was carried out in Poland, and it had the aim of determining the exhalation flow of radon in the soil with the help of Lucas cells. The cells were connected through a desiccant tube to an accumulation chamber with a diameter of 35 cm and a height of 20 cm. Radon gas accumulated for 2.5 h. After this period of time, the accumulated gas was sent through the Lucas cell with the help of a pump, and the radon concentration was measured. Swakoń et al. [18] determined the soil radon concentration in the disjunctive tectonic zones of Krakow. The soil radon concentration was measured by an Alpha Guard PQ2000 PRO device at a depth of 1 m. They also determined the radon concentration with a passive method using CR-39 trace detectors that were placed inside an aluminium pipe at the same depth. These detectors were collected and analysed through a method developed by the Institute of Nuclear Physics in Krakow.

In Austria, Friedmann et al. [19] evaluated the radon concentration in the soil using Alpha Guard (Genitron Instruments, Frankfurt, Germany) and Atmos 12 DPX (Gammadata, Uppsala, Sweden). The approach utilised three sampling points representing the corners of an equilateral triangle having 1.5 m sides. The authors used the protocol published by Neznal et al. [13] to compute the GRP. Mancini et al. [20] measured the radon concentration in soil with the RAD7 device at a minimum depth of 0.7 m. The arithmetic mean for 95 measurements was 13.75 kBq/m<sup>3</sup> and a standard deviation of 1.48 kBq/m<sup>3</sup> with a maximum of 90 kBq/m<sup>3</sup>.

In Romania, Florică et al. [21] determined GRP on construction sites using the Neznal method. Using RM-2 (Radon v.o.s., Czech Republic) and Radon Jok, respectively, radon concentration and soil permeability were measured. Cosma & Baciu [22] determined the radon activity concentration using a LUK3A device at a depth of 0.7 m. In this case, the soil permeability was estimated. The distance to the granite massif of Maguri-Racatau was taken into account. It could be observed that at short distances to this massif, the soil radon concentrations were lower. At distances of 7.1 km, the radon concentrations were as high as 81 kBq/m<sup>3</sup>, with concentrations of about 61 kBq/m<sup>3</sup> in Apahida village. Lupulescu et al. [23] measured a monthly variation of soil radon concentration. The geogenic radon concentration was measured with a LUK3C device. The soil permeability was measured with a Radon Jok device. This study took place over a period of seven

months, from December to June, and it took into account meteorological conditions, such as temperatures, pressure, air humidity, and speed. The authors determined an inverse proportionality relation between soil radon concentration and atmospheric pressure. It was also determined that radon concentration is inversely proportional to soil permeability. The radon index was medium for each month, even though the soil radon concentration varied from 16.6 to 32.2 kBq/m<sup>3</sup>. Burhele et al. [24] gathered information from different measurement campaigns carried out by their team between 2012 and 2018. Data were published according to JRC's (Joint Research Centre) methodology. Radon concentration was measured at a depth of 0.8 m with a LUK3C device.

Kemski et al. [7,25] applied an empirical method to determine the GRP in Germany. The radon concentration was measured using Lucas cells connected to a steel probe inserted in the soil at a depth of 1 m. The soil permeability was measured using a permeameter connected to the same probe. Measurements were performed at three points that created an isosceles triangle with a base of 5 m and a height of 5 m. When determining GRP, the maximum radon concentration and the average soil permeability at three points were considered, and a radon ranking matrix was applied. The authors divided the GRP into classes based on radon concentration and soil permeability: classes 1 to 6 (local scales) and classes A to E (regional scales).

Giustini et al. [26] calculated the GRP in a volcanic region of central Italy using Empirical Bayesian Kriging regression. The radon concentration in soil gas was determined using RAD7 and a single sampling probe connected to a drying tube. In another Italian study, Ciotoli et al. [9] estimated GRP using regression models OLS (ordinary least squares) and GWR (geographically weighted regression). The authors considered the digital terrain model (DTM), the map of the homogeneous geological units, the map of the major faults, the map of the hydrogeological complexes, and the map of the soil gas radon concentrations. Radon concentration was measured using an active radon detector equipped with a different Lucas cell for every measuring point. The permeability of the soil was estimated using the hydrogeological map.

Alonso et al. [27] utilised RAD7 to determine radon concentration and Radon Jok to determine soil permeability at a single measurement point in the Eastern Canary Islands. GRP was calculated with the Neznal method.

Measuring the geogenic radon potential over broad areas requires a significant amount of time and labour; consequently, it is vital to establish a simple procedure that maximises the accuracy of the results. Starting from the protocol developed by Neznal et al. [13], the present study aims to test different layouts of the measuring points in order to identify the optimal calculation method, which will provide a balance between the accuracy of the results and the optimisation of working time and effort per location. This study is a step forward in the standardisation of methods at an international level when calculating the geogenic radon potential when the concentration of radon activity in the soil is measured with the RM-2 device in any location, not only for building sites.

## 2. Materials and Methods

**Site description.** The Poiana Rusca Mountains (Hunedoara County, Romania) are situated at the northwestern extremity of the Southern Carpathians (between 45°55' and 45°30' N and 22° and 23° E) and have a total area of about 2640 km<sup>2</sup>. The Poiana Rusca Mountains are bounded by the Mures River and the Metaliferi Mountains to the north and by the Bistra Valley to the south. To the west, the Poiana Rusca massif is bordered by the Caransebes Depression and to the East by the Hateg and Strei Depressions [28].

From a morphological point of view, the study region is an intramountain depression surrounded by heights that reach 1009 m (Alunului Peak) in the northern part and 1000 m in the southern part. The exceptionally humid climate has allowed numerous springs to form in this region, springs that feed the permanent watercourses; their erosional activity is pronounced and profound [29].

The particular research location surrounding the village of Lunca Cernii was chosen based on the high levels of radon emission from soil observed during early field surveys and the geological substrate's variability, which occurs across a relatively small area. It corresponds to the eastern portion of the Rusca Montana sedimentary area, which is a SW–NE syncline filled with Cretaceous deposits superposed on an Upper Proterozoic–Lower Paleozoic crystalline basement [30]. Upper Proterozoic medium-grade metamorphic rocks of the Sebes-Lotru Series outcrop to the north and south of the sedimentary area. It was divided into two sub-series: biotite paragneiss at the base, followed by mica schist with almandine [31,32]. Some small magnetite-bearing lenses have been mined in the past as iron ore. The epimetamorphic Dabaca series outcrops eastward from the sedimentary basin and mainly consists of muscovite or sericite schists, amphibolites, and crystalline limestone. Its inferred age is Upper Proterozoic–Lower Paleozoic (Cambrian). The metamorphic rocks are intensely folded and fractured. The Lunca Cernii synform extends northeastward from the sedimentary area, while the Voislova-Silvas antiform runs parallel to the synform and about 2 km to its south. The major faults, Lunca Cernii–Lingina and Rusca Montana–Hasdau, are also parallel to the plication elements. The latter marks the boundary between the Cretaceous sediments and the Sebes-Lotru metamorphics.

The Rusca Montana–Lunca Cernii syncline hosts Mesozoic deposits, starting with some Jurassic sequences to the west [33], which are absent from our research region. In our area of interest, sediments from the Cretaceous period (Barremian–Cenomanian–Santonian–Maastrichtian) cover the crystalline basement. They are composed primarily of detrital sediments with occasional carbonate packages. The Maastrichtian includes two volcano-sedimentary sequences, with andesite lava and breccia intercalations. Some detrital sediments, Paleogene [32] or Lower Miocene [34], occur on top of the sedimentary pile. The syncline is affected by a major longitudinal fault. Along the region's major streams, Quaternary coarse detrital sediments are present.

Measurement of radon activity concentration in soil gas and soil permeability. In 34 locations of the Rusca Montana Basin, an RM-2 (Radon v.o.s., Czech Republic) device was used to assess the radon content in the soil. The device consists of several IK-250 ionisation chambers, an ERM-3 reader, and a soil-gas sampling set. Steps to determine the radon activity concentration in the soil include the following:

- The ionisation chambers are vacuumed using a manual or electric pump;
- The gas sampling probes (steel pipes) are introduced in the soil at a depth of 80 cm;
- The gas from the soil is sampled using a 150 mL Janet syringe connected to the sampling probes;
- The gas sample is introduced in the ionisation chamber. Following this step, 50 mL of ambient air is introduced into the ionisation chamber to reach a total volume of 200 mL;
- In order to eliminate any trace of thoron, the sample is left to rest for 15 min;
- After 15 min, the ionisation chamber is connected to the ERM-3 electrometer and radon activity concentration is measured. The alpha radiation emitted by radon in the ionisation chamber creates an ionisation current, which is measured for 120 s;
- After 120 s, the ERM-3 electrometer displays the radon activity concentration in volume activity units (kBq/m<sup>3</sup>) [35].

The soil permeability was assessed using a Radon Jok device (Radon v.o.s., Czech Republic). The Radon Jok was equipped in the upper part with an expandable air cell with a total volume of  $2 \times 10^{-3} \text{ m}^3$ . In the upper part of the air cell, there was a tap connected to the soil air extraction probe, and in the lower part of the cell, there was a calibrated metal rod. On the opposite side of the expandable air cell, on the metal rod, two weights were positioned in order to extend the air cell with the sampled air. The pressure difference was 2160 Pa when using only one weight during the permeability measurement and 3750 Pa when using both weights. In the lower part, the Radon Jok device was equipped with a tripod for correct use in the right vertical position. The radon activity concentrations and soil permeability were measured at a depth of 0.80 metres. Darcy's equation [36] provided

the basis for permeability assessment. Participation in frequent intercomparison exercises regarding soil radon measurements at the Czech Republic reference locations [37] ensured the quality of the measurements.

At each of the 34 sites, 15 measurements were performed. On the basis of these 15 measurements, various measuring schemes, depicted in Figure 1 and comprising different numbers of points, were selected. Thus, four distinct configurations with three points (3.1, 3.2, 3.3, 3.4) were chosen, as well as one configuration, each with five, nine, and fifteen points. The distance between two neighbouring points was set between 3 and 5 m, based on the local morphology, but remained consistent at each location. Each sampling site covered an area of 120–150 m<sup>2</sup>. Using Equation (1), the original method proposed by Neznal et al. [13] was utilised to compute the geogenic radon potential (GRP):

$$GRP = \frac{3^{rd} \text{ quartile of Radon Concentration in Soil} - 1}{-\log(3^{rd} \text{ quartile of Soil Permeability}) - 10} \tag{1}$$

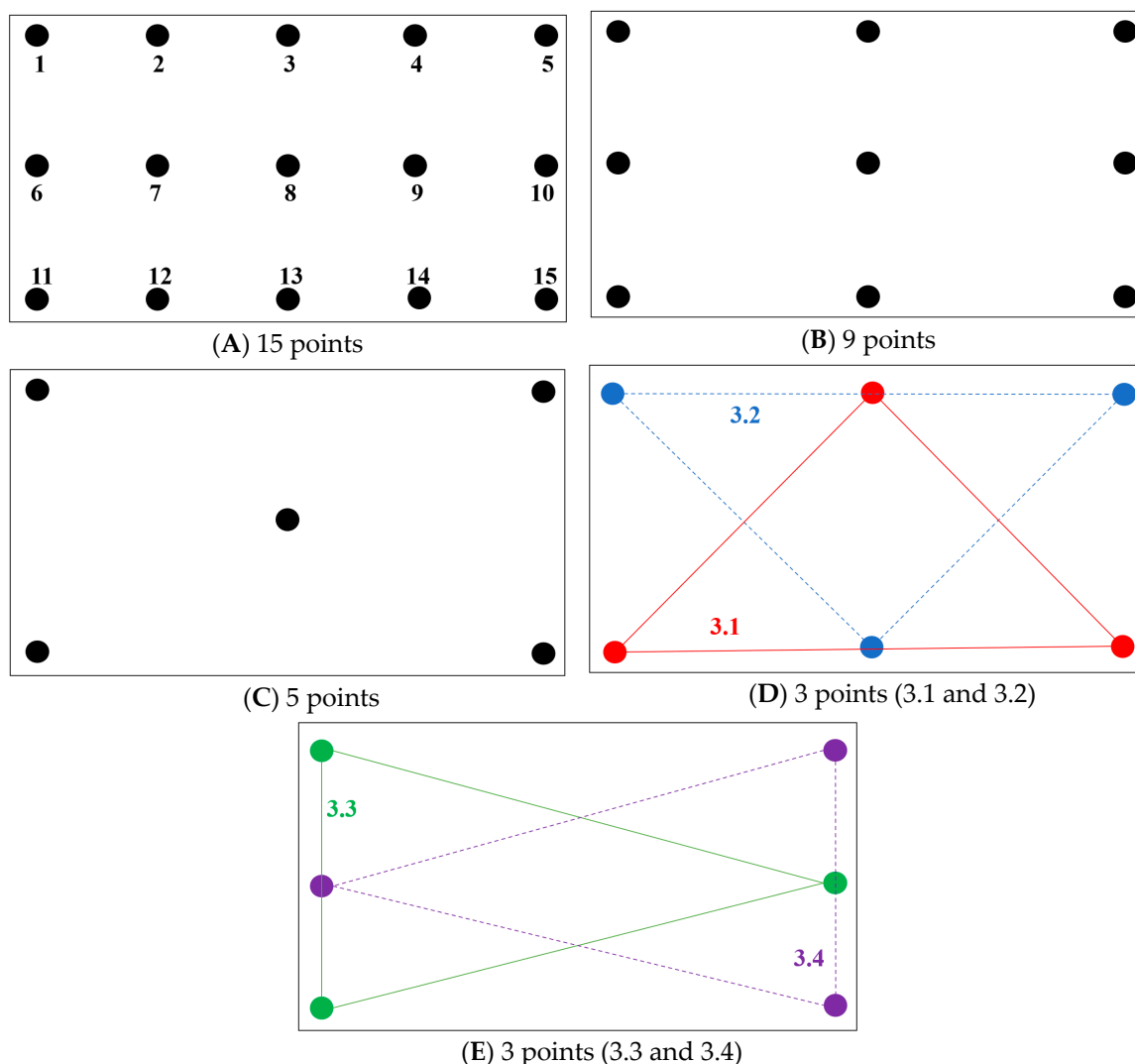


**Figure 1.** The measurement scheme depending on the number of points for each location.

Data analysis. Statistical analysis of the data was performed using IBM SPSS Statistics software, version 24 (SPSS Inc., Chicago, IL, USA). As a result, the ANOVA test for repeated measurements with Tukey posthoc analysis was chosen to compare the findings obtained from the various measurement strategies. The test is used to assess the significance of

differences between pairs of group means and was applied to log-transformed data [38]. The GRP calculated for the layout with 15 measuring points was chosen as a reference. Therefore, the *t*-test for paired data or non-parametric Wilcoxon matched-pairs signed rank test was used. This test compares the median of a set of numbers against a hypothetical median [39]. The significance level was chosen at  $\alpha = 0.05$ . Furthermore, the intraclass correlation coefficient (ICC) was utilised to examine the level of correlation and agreement between measurement systems. In this sense, the single-measurement, absolute-agreement, 2-way mixed-effects model was applied. The interpretation of the ICC was based on the recommendation of Koo et al. [40].

### 3. Results and Discussion

For the 510 measurements (34 locations with 15 measurements each), the radon concentration in the soil had an arithmetic mean of 31.9 kBq/m<sup>3</sup> and a geometric mean of 27.7 kBq/m<sup>3</sup>; the minimum measured radon concentration was 0.2 kBq/m<sup>3</sup>, with a highest concentration of 93.7 kBq/m<sup>3</sup>. The dispersion of the radon concentrations, evaluated with the coefficient of variation, indicated a value of 51%. In a study conducted in 16 counties in the central-northwestern region of Romania, Burghel et al. [24] found a range between 0.2 and 179 kBq/m<sup>3</sup> for the 2564 soil radon readings. In the study of Ciotoli et al. [9], the average radon concentration in soil from Italy’s Lazio region ranged from 14 to 85 kBq/m<sup>3</sup>. Giustini et al. [26] reported values ranging from 6.4 to 253 kBq/m<sup>3</sup>, with an average of 60 kBq/m<sup>3</sup> at 184 locations in a central Italy volcanic region.

In the present study, the arithmetic mean of soil permeability was  $7.71 \times 10^{-12}$  m<sup>2</sup>, with a minimum value of  $5.59 \times 10^{-13}$  and a maximum value of  $2.19 \times 10^{-11}$ . The calculated GRP for each location was based on Equation (1), using the soil radon concentration and soil permeability data obtained. Table 1 provides descriptive GRP statistics for various measurement schemes. The 15-point measurement scheme was used as a reference. Thus, the arithmetic mean GRP for this measurement was 37, with a geometric mean of 33 and a variation between 12 and 110. In the study conducted by Florică et al. [21], the GRP ranged from 5 to 133, with a median of 29 and an average of 33 for 100 locations in five Romanian cities. Szabo et al. [15] determined that the GRP ranged from 1 to 74 across 192 locations in Hungary, with a mean of 12 and a median of 8.

**Table 1.** The descriptive statistics for different measurement schemes for GRP in 34 locations.

Measurement Scheme <sup>1</sup>	ICC (95% CI) <sup>2</sup>	Min. <sup>3</sup>	Max.	A.M.	S.D.	G.M.	Median	CV (%)
15		12	110	37	20	33	32	54
9	0.96 (0.93–0.98)	11	113	38	21	33	33	56
5	0.85 (0.73–0.92)	12	100	36	19	32	33	52
3.1	0.83 (0.67–0.92)	8	83	33	18	29	28	55
3.2	0.79 (0.61–0.89)	9	75	37	17	33	32	45
3.3	0.77 (0.59–0.88)	11	69	34	15	31	33	45
3.4	0.89 (0.80–0.95)	6	124	36	23	31	31	61

<sup>1</sup> 15—GRP for 15 points; 9—GRP for 9 points; 5—GRP for 5 points; 3.1, 3.2, 3.3, 3.4—GRP for 3 points; <sup>2</sup> ICC between 15 points measurement scheme and tested scheme; <sup>3</sup> Min.—minimum; Max.—maximum; A.M.—arithmetic mean; S.D.—standard deviation; G.M.—geometric mean; CV (%)—coefficient of variation.

The ANOVA test applied to log-transformed data for repeated measurements revealed no statistically significant difference ( $p > 0.05$ ) between the measurement schemes depicted in Figure 1. By applying the *t*-test for paired data, the average difference between each

measurement scheme and the one with 15 points was not significantly different from zero ( $p > 0.05$ ), except for configuration 3.1 ( $p = 0.02$ ). Applying the non-parametric Wilcoxon matched-pairs signed rank test yielded similar results.

Excellent reliability between the 15- and 9-point measurement schemes was found through ICC = 0.96 (95% CI: 0.93–0.98). The ICC value for the five-point measuring scheme was 0.85, while the 95% confidence range showed a moderate to good degree of reliability. For the four selected configurations with three measurement points, the ICC values ranged from 0.77 (scheme 3.3) to 0.89 (scheme 3.4), with the associated 95% confidence interval indicating moderate to good reliability. Comparing measuring schemes that do not contain the same points (such as scheme 3.1 with scheme 3.2 or scheme 3.3 with scheme 3.4) yielded an ICC value of 0.70 and 0.65, respectively, with a confidence interval ranging from low (0.4) to good (0.81). For the five-point scheme presented in Figure 1C and alternative schemes that targeted five other distinct points (2, 4, 6, 12, and 14 or 3, 6, 10, 12, and 13), the ICC showed a confidence interval between 0.50 and 0.94, indicating reliability between moderate and excellent. For the scheme with 9 measurement points, a comparison was made with a similar scheme as the number of points; as only 15 points were measured per location, in this case, 3 points were shared. The ICC value for this arrangement was 0.86, with a 95% confidence interval between 0.75 and 0.93.

The calculated GRP values resulted in a moderate radon index for 23 locations and a high radon index for 11 locations. No location within the research region was found to have a low radon index.

Table 2 displays the descriptive statistics for radon concentration in soil, soil permeability, and GRP for 15 measurement points within each geological formation.

**Table 2.** The descriptive statistics of radon concentration, soil permeability, and geogenic radon potential in seven geological units, according to the 15-measurement points scheme.

Geological Unit	No. Meas.	Radon Concentration (kBq/m <sup>3</sup> )			Soil Permeability (m <sup>2</sup> )	GRP			
		Min.	A.M.	Max.	A.M.	Min.	A.M.	Max.	CV(%)
Formation of sericitic quartzite schists with amphibolite intercalations (Dabaca series)	2	15.6	27.5	62.2	$2.53 \times 10^{-12}$	13	17	20	45
Micaceous schists formation with amphibolite intercalations (Dabaca series)	1	19.2	30.7	42.7	$5.49 \times 10^{-12}$	-	29	-	-
Micaschists with almandine (Sebes-Lotru series)	5	21.2	34.8	53.2	$4.38 \times 10^{-12}$	14	25	42	48
Sedimentary cover Rusca Montana Dep.	16	14.8	30.8	54.5	$7.95 \times 10^{-12}$	11	33	90	53
Sedimentary alluvium	3	17	35.2	56.8	$5.33 \times 10^{-12}$	27	31	39	55
Bautar Formation	4	26.7	37.9	54.1	$1.26 \times 10^{-11}$	25	40	67	28
Voislova Formation	3	12.3	25.0	40.8	$1.20 \times 10^{-11}$	26	30	33	44

A high geogenic radon potential was detected in the Bautar Formation (arithmetic mean = 40), which consists primarily of biotite paragneiss with almandine, staurolite, or disten, intercalated with crystalline limestone, amphibolites, and rare magnetite lenses. It was determined that the Dabaca formation, composed of sericite quartzite schists with amphibolite intercalations, has a low geogenic radon potential (arithmetic mean = 17).

Most of these measurements were carried out in the sedimentary cover Rusca Montana Depression. In terms of radon activity concentration in soil, the Upper Precambrian–Lower Palaeozoic Formation of sericite quartzite schists included in the Dabaca series ( $62.2 \text{ kBq/m}^3$ ) and the sedimentary alluvium ( $56.8 \text{ kBq/m}^3$ ) had the highest values. The lowest concentration of radon activity was determined in the Voislova formation ( $12.3 \text{ kBq/m}^3$ ). The soil permeability was high in most of the measuring points. It appeared to be lower in certain alluvial areas (Lunca Cernii de Jos, Negoiu, Gura Bordului) because of the high hydrostatic level, which brings groundwater close to the surface, hence reducing soil permeability ( $5.59 \times 10^{-13} \text{ m}^2$ ). The coefficient of variation for the sedimentary alluvium was high (55%), while the Bautar Formation coefficient was low (28%).

Figure 2 shows the distribution of the radon index among the 34 sites in relation to the underlying geology. A higher geogenic radon potential was observed in the area of sedimentary deposits with volcanoclastic intercalations from the Cretaceous–Paleogene sedimentary cover of Rusca Montana, as well as in the area of the Bautar Formation, which belongs to the Prebaikal cycle (Upper Precambrian). A lower GRP was found in the Dabaca series area (Upper Precambrian–Cambrian). In the Micaschists with almandine formations, the geogenic radon potential was determined only in one out of the five locations in the northern part of the study area.

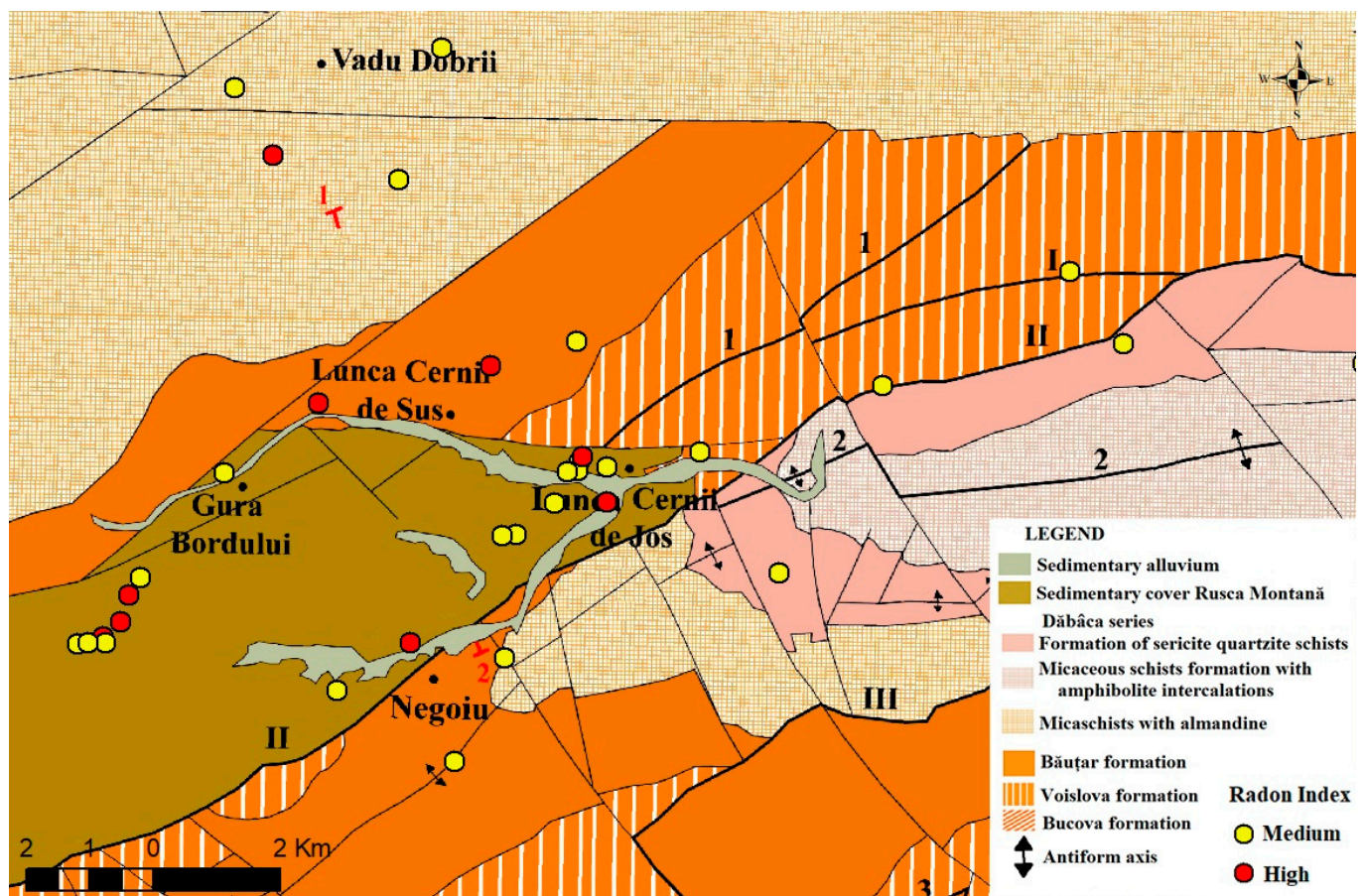


**Figure 2.** The distribution of measurement points and the radon index in the study area against the geological background, after Maier et al. [32].

#### 4. Conclusions

Based on the *t*-test and Wilcoxon test, there was no statistically significant difference for the method between 15 and 9, 5, 3 measurement points, except for one configuration (3.1). A single measurement point of radon concentration is not recommended for the RM-2 device. Human and technical errors may occur; thus, the value of the radon concentration

determined may differ from its actual value. A minimum of three radon concentration and soil permeability measurements will enhance the data quality. According to the results obtained in terms of ICC, even when measurement schemes were chosen in such a way that targeted different points at each site, a five-point measurement scheme led to moderate reliability, whereas measurement schemes with nine and more points exhibited good to excellent reliability.

The meticulousness of geogenic radon measurements should be a function of purpose. If mapping the geogenic radon potential as a function of geology is the objective, then three measurements per location may be sufficient. Thus, the time necessary to determine the geogenic radon potential can be decreased from 4.5 to 5 h for 15 measurement points to between 45 min and one hour for 3 measurement points. More measuring points for each location should only be required for general radon surveys if the radon concentration and soil permeability at each location are highly heterogeneous.

**Author Contributions:** A.L.—conceptualisation, methodology, investigation; C.B.—geology, conceptualisation, review and editing; T.D.—software, conceptualisation, statistics, review and editing; B.-D.B.—review and editing; A.L.C.—review and editing. All authors have read and agreed to the published version of the manuscript.

**Funding:** The present work has received financial support through the projects: Entrepreneurship for innovation through doctoral and postdoctoral research, POCU/380/6/13/123886 co-financed by the European Social Fund, through the Operational Program for Human Capital 2014–2020; by a grant of the Ministry of Research, Innovation and Digitization, CNCS-UEFISCDI, project number PNIII-P1-1.1-TE-2021-0249, within PNCDI III and also by the project ID P\_37\_229, Contract No. 22/1 September 2016, with the title, “Smart Systems for Public Safety through Control and Mitigation of Residential Radon linked with Energy Efficiency Optimization of Buildings in Romanian Major Urban Agglomerations SMART-RAD-EN” of the POC Programme.

**Institutional Review Board Statement:** Not applicable.

**Informed Consent Statement:** Not applicable.

**Data Availability Statement:** The data that support the findings of this study are available from the corresponding author, upon reasonable request.

**Conflicts of Interest:** The authors declare no conflict of interest.

## References

1. Cosma, C.; Cucos (Dinu), A.; Dicu, T. Preliminary Results Regarding the First Map of Residential Radon in Some Regions in Romania. *Radiat. Prot. Dosim.* **2013**, *155*, 343–350. [[CrossRef](#)] [[PubMed](#)]
2. Dai, D.; Neal, F.B.; Diem, J.; Deocampo, D.M.; Stauber, C.; Dignam, T. Confluent Impact of Housing and Geology on Indoor Radon Concentrations in Atlanta, Georgia, United States. *Sci. Total Environ.* **2019**, *668*, 500–511. [[CrossRef](#)] [[PubMed](#)]
3. *IARC Monographs on the Evaluation of the Carcinogenic Risks to Humans*; International Agency for Research on Cancer: Lyon, France, 1988.
4. Monitorul Oficial HG 526/2018—Planul Național de Acțiune La Radon; Nr. 645/25.VII.2018; Monitorul Oficial: Bucharest, Romania, 2018; (*Official Gazette HG 526/2018—The national radon action plan*; No. 645/25.VII.2018).
5. EURATOM 59 Council Directive 2013/59/Euratom of 5 December 2013 Laying down Basic Safety Standards for Protection against the Dangers Arising from Exposure to Ionising Radiation, and Repealing Directives 89/618/Euratom, 90/641/Euratom, 96/29/Euratom, 97/43/Euratom; EURATOM: Rome, Italy, 2013.
6. Nero, A. Earth, Air, Radon and Home. *Phys. Today* **1989**, *42*, 32–39. [[CrossRef](#)]
7. Kemski, J.; Siehl, A.; Stegemann, R.; Valdivia-Manchego, M. Mapping the Geogenic Radon Potential in Germany. *Sci. Total Environ.* **2001**, *272*, 217–230. [[CrossRef](#)] [[PubMed](#)]
8. Kemski, J.; Klingel, R.; Siehl, A.; Stegemann, R. Radon Transfer from Ground to Houses and Prediction of Indoor Radon in Germany Based on Geological Information. *Radioact. Environ.* **2005**, *7*, 820–832. [[CrossRef](#)]
9. Ciotoli, G.; Voltaggio, M.; Tuccimei, P.; Soligo, M.; Pasculli, A.; Beaubien, S.E.; Bigi, S. Geographically Weighted Regression and Geostatistical Techniques to Construct the Geogenic Radon Potential Map of the Lazio Region: A Methodological Proposal for the European Atlas of Natural Radiation. *J. Environ. Radioact.* **2017**, *166*, 355–375. [[CrossRef](#)]
10. Bossew, P. Mapping the Geogenic Radon Potential and Estimation of Radon Prone Areas in Germany. *Radiat. Emerg. Med.* **2015**, *4*, 13–20.
11. Appleton, J.D. Radon: Sources, Health Risks, and Hazard Mapping. *Ambio* **2007**, *36*, 85–89. [[CrossRef](#)]

12. Cinelli, G.; Tollefsen, T.; Bossew, P.; Gruber, V.; Bogucarskis, K.; De Felice, L.; De Cort, M. Digital Version of the European Atlas of Natural Radiation. *J. Environ. Radioact.* **2019**, *196*, 240–252. [[CrossRef](#)]
13. Neznal, M.; Neznal, M.; Matolin, M.; Barnet, I.; Miksova, J. *The New Method for Assessing the Radon Risk of Building Sites*; Czech Geological Survey: Praga, Czech Republic, 2004.
14. Mikšová, J.; Barnet, I. Geological Support to the National Radon Programme (Czech Republic). *Bull. Czech Geol. Surv.* **2002**, *77*, 13–22.
15. Szabó, K.Z.; Jordan, G.; Horváth, Á.; Szabó, C. Mapping the Geogenic Radon Potential: Methodology and Spatial Analysis for Central Hungary. *J. Environ. Radioact.* **2014**, *129*, 107–120. [[CrossRef](#)]
16. Planinić, J.; Vuković, B.; Radolić, V.; Stanić, D. Radon in Soil and Homes of Osijek. In Proceedings of the European IRPA Congress, Florence, Italy, 8–11 October 2002; p. 37, ISBN 88-88648-09-7.
17. Chalupnik, S.; Wysocka, M. Measurement of Radon Exhalation from Soil—Development of the Method and Preliminary Results. *J. Min. Sci.* **2003**, *39*, 191–198. [[CrossRef](#)]
18. Swakoń, J.; Kozak, K.; Paszkowski, M.; Gradziński, R.; Łoskiewicz, J.; Mazur, J.; Janik, M.; Bogacz, J.; Horwacik, T.; Olko, P. Radon Concentration in Soil Gas around Local Disjunctive Tectonic Zones in the Krakow Area. *J. Environ. Radioact.* **2005**, *78*, 137–149. [[CrossRef](#)]
19. Friedmann, H.; Baumgartner, A.; Bernreiter, M.; Gräser, J.; Gruber, V.; Kabrt, F.; Kaineder, H.; Maringer, F.J.; Ringer, W.; Seidel, C.; et al. Indoor Radon, Geogenic Radon Surrogates and Geology—Investigations on Their Correlation. *J. Environ. Radioact.* **2017**, *166*, 382–389. [[CrossRef](#)]
20. Mancini, S.; Guida, M.; Cuomo, A.; Guida, D. A Geogenic Approach for the Radon Monitoring and the Exposure Assessment at a Regional Scale: The Results of the Rad\_Campania Project. *Adv. Geosci.* **2020**, *52*, 87–96. [[CrossRef](#)]
21. Florică, Ș.; Burghele, B.D.; Bican-Brișan, N.; Begy, R.; Codrea, V.; Cucuș, A.; Catalina, T.; Dicu, T.; Dobrei, G.; Istrate, A.; et al. The Path from Geology to Indoor Radon. *Environ. Geochem. Health* **2020**, *42*, 2655–2665. [[CrossRef](#)]
22. Cosma, C.; Baciuc, C. Dinamica Radonului. In *Municipiul Cluj-Napoca și zona periurbană—Studii ambientale*; Editura Accent: Cluj-Napoca, Romania, 2002; (*Radon dynamics. In the Cluj-Napoca City and peri-urban area—Environmental studies*).
23. Lupulescu, A.; Dicu, T.; Papp, B.; Cucos, A. Determination of the Monthly Variation of Radon Activity Concentration in Soil. *Stud. Univ. Babeș Bolyai Ambient.* **2018**, *63*, 49–59. [[CrossRef](#)]
24. Burghele, B.; Țenter, A.; Cucuș, A.; Dicu, T.; Moldovan, M.; Papp, B.; Szacsvai, K.; Neda, T.; Suciuc, L.; Lupulescu, A.; et al. The FIRST Large-Scale Mapping of Radon Concentration in Soil Gas and Water in Romania. *Sci. Total Environ.* **2019**, *669*, 887–892. [[CrossRef](#)]
25. Kemski, J.; Klingel, R.; Siehl, A. Classification and Mapping of Radon-Affected Areas in Germany. *Environ. Int.* **1996**, *22*, 789–798. [[CrossRef](#)]
26. Giustini, F.; Ciotoli, G.; Rinaldini, A.; Ruggiero, L.; Voltaggio, M. Mapping the Geogenic Radon Potential and Radon Risk by Using Empirical Bayesian Kriging Regression: A Case Study from a Volcanic Area of Central Italy. *Sci. Total Environ.* **2019**, *661*, 449–464. [[CrossRef](#)]
27. Alonso, H.; Rubiano, J.G.; Guerra, J.G.; Arnedo, M.A.; Tejera, A.; Martel, P. Assessment of Radon Risk Areas in the Eastern Canary Islands Using Soil Radon Gas Concentration and Gas Permeability of Soils. *Sci. Total Environ.* **2019**, *664*, 449–460. [[CrossRef](#)]
28. Krautner, H. *Munții Noștri: Poiana Ruscă*; Editura Sport-Turism: București, Romania, 1984; (*Our mountains: Poiana Rusca*).
29. Mamulea, A. Cercetări Geologice În Regiunea Rusca Montană—Lunca Cernii: Ședința Din 21 Martie 1952. *Dări de seamă ale sedintelor* **1952**, *39*, 172–178, (*Geological research in the Rusca Montana—Lunca Cernii Region*).
30. Balintoni, I.; Iancu, V. Probleme de Metamorfism, Litostratigrafie Si Structura Ale Cristalinului Din Masivul Poiana Rusca. *Studii si cercetari de Geologie Geofizica Geografie Seria de geologie* **1986**, *31*, 51–67, (*Problems of Metamorphism, Lithostratigraphy and Crystalline Structure from the Poiana Rusca Massif*).
31. Maier, O.; Solomon, I.; Zimmermann, P.; Zimmermann, V. Studiul Geologic Și Petrografic al Cristalinului Din Partea Sudică a Munților Poiana Ruscă. *Anuarul Institutului Geologic și Geofizic* **1975**, *43*, 65–189, (*The Geological and Petrographic study of the Crystalline from the Southern Side of the Poiana Rusca Mountains*).
32. Maier, O.; Lupu, M. *Harta Geologică Republica Socialistă România, Scara 1:50.000, Foaia 105a, Băuțar*; Institutul de Geologie și Geofizică: București, Romania, 1979; (*Geological map of the Socialist Republic of Romania, Scale 1:50000, Sheet 105a, Băuțar*).
33. Dincă, A. Geologia Bazinului Rusca Montană. Partea de Vest. *Anu. Inst. De Geol. și Geofiz.* **1977**, *52*, 99–173, (*Geology of the Rusca Montana Basin. Western Part*).
34. Codarcea, A.; Dimitrescu, R.; Gherasi, N.; Mureșan, M.; Mureșan, G.; Krautner, H.; Krautner, F.; Lupu, M.; Marinescu, F.; Savu, H.; et al. *Harta Geologică a Republicii Socialiste România, Scara 1:200.000, L-34-XXIII 25, Deva*; Comitetul de Stat pentru Geologie. Institutul Geologic: București, Romania, 1968; (*Geology of the Rusca Montana Basin. Western Part*).
35. Radon—Measurements, research, protection, equipment. Available online: <https://radon.eu/rm2.html> (accessed on 21 January 2023).
36. Neznal, M.; Neznal, M. Determination of Soil-Gas Radon Concentration in Low Permeability Soils. *Radioact. Environ.* **2005**, *7*, 722–725. [[CrossRef](#)]
37. Matolin, M. *International Comparison Measurement of Radon in Soil Gas at Radon Reference Sites Cetyne and Buk in the Czech Republic*; Publisher: Prague, Czech Republic, 2021.
38. Tukey, J.W. Comparing Individual Means in the Analysis of Variance. *Biometrics* **1949**, *5*, 99. [[CrossRef](#)]

39. Wilcoxon, F. Individual Comparisons by Ranking Methods. *Biom. Bull.* **1945**, *1*, 80–83. [[CrossRef](#)]
40. Koo, T.K.; Li, M.Y. A Guideline of Selecting and Reporting Intraclass Correlation Coefficients for Reliability Research. *J. Chiropr. Med.* **2016**, *15*, 155–163. [[CrossRef](#)] [[PubMed](#)]

**Disclaimer/Publisher’s Note:** The statements, opinions and data contained in all publications are solely those of the individual author(s) and contributor(s) and not of MDPI and/or the editor(s). MDPI and/or the editor(s) disclaim responsibility for any injury to people or property resulting from any ideas, methods, instructions or products referred to in the content.